Identification Of The Relative Active Neo-Tectonic Variation In The Chel Basin Based On Morphometry And Physical Characteristics Of The Sedimentary Facies, North Bengal, India

[1]Ramapada Sasmal, [2]Dr Soma Bhattacharya

[1]Research scholar, Department of Geography, Vivekananda College for Women, University of Calcutta and Assistant Professor, Arambagh Girls' College, University of Burdwan, West Bengal, India. Phone: +91 6294897700,
[1]Principal, Vivekananda College for Women, University of Calcutta, West Bengal, India.Phone: +91 9874220701,

---

Abstract: *The tourism and tea plantation is the backbone of economy of the Chal River basin. But, the neo-tectonic activities causes landslide and gully erosion, which are the main obstacle of the said economic activities of this basin area. The Main Central Thrust (MCT), Ramgarh Thrust (RT), Main Boundary Thrust (MBT), Main Frontal Thrust (MFT), and Ghish Travers Zone (GTZ) are the major tectonic signature in this basin. The neo-tectonic activities of this thrust contacts is not homogeneous throughout the basin area. The identification of the neo-tectonic variation of those thrust contacts is the main aim of this article. To identify this variation the measurement and analysis of the morphometry of relief, basin area and drainage networks and the identification and measurement of sedimentology are the main objective of this study. In this purpose SRTM DEM data of the USGS are analyzed with the help of GIS software and the tectonic terrace, area of headword erosion of the streams and the physical properties of the sedimentary facies are examined in the field. Analysis found a prominent break in slope near RT, highly elongated nature of the 2nd and 3rd order sub-basin, circular sub-basin in the north of MCT, presence of headword erosion near MBT, alteration of coarse and fine grain sedimentary facies in the south of RT, scale like foliation of phyllaite near RT, presence of boulder facies in the flood plain area etc. All the observation advocates for relatively inactive or negligibly active nature of MCT and MFT, active nature of RT and GTZ, and gradual reactivation of MBT in the study area.*

Keywords: Morphometry, Sub-basin, Neo-tectonic, Thrust contact, Facies, Sinuosity

1. INTRODUCTION

Neo-tectonic is a problem in the Chel River basin. Because, neo-tectonic deformation causes landslide and gully erosion, which makes an obstacle in the plantation of tea and growth of the tourism industry. The tea is cultivated here both in the mountain surface and low fun area. But, the neo-tectonic activities causing gully erosion accelerate soil erosion, which hampers the tea plantation mainly in mountain terrain. However, the Lava Road stretches through the central axis of this basin in a north-south direction. The landslide along this road at a lower attitudinal area hampers the flow of tourists in this area. Alternatively, neo-tectonics reshape the sub-basins, which cause flood and resultant hampering of crop cultivation in the lower basin area. So, the Chel basin needs to the identification of the variation of tectonic impact on its different parts for the remedial measure of the aforesaid problems.

Eminent scholars worked out on the tectonics, geology and drainage system of the Himalayas. Latitudinal division of the Himalayas has been done based on geology and geotectonic (Heim, A. and Gansser, A., 1939; Yin, A., 2006; Valdiya, K. S. 2002). The study of regional tectonic setting in the Darjiling–Sikkim–Tibet (DaSiT) Himalayan wedge has been conducted (Mitra, G. et al., 2010; Mukul, M. et al. 2014). Some micro-level studies on MCT (Yin, A. 2006; Srivastava, V. et al., 2017), RT (Pearson, O. N. and DeCelles, P. G., 2005; Mukul, M., 2010; Mitra, G. et al. 2010; Matin and Mukul, 2010), MBT (Nakata, T.,1989; Mohapatra, S. R. et al., 2012; Srivastava, V., 2017) and MFT (Geddes, 1960; Mohapatra, S. R. et al., 2012; Srivastava, P. and Mitra, G., 1994; DeCelles, P. G., Gehrels, G. E., Quade, J. and Ojha, T. P., 1998.) have been done in this region. Most geomorphologists pay attention to the middle and western Himalayas to study the drainage system. Few geomorphologists studied major rivers in the eastern Himalayas (Basu and Sarkar,1990; Bhattacharya, S.; 2004; Chakraborty and Ghosh, 2010; Chakraborty et al., 2013; Chakraborty and Mukhopadhyay, 2014; Fergusson, 1863; Guha et al., 2007; Morgan and Mc Intire, 1959).

However, the river Chel is flowing through a tectonic lineament (Dasgupta et al., 2000). Only Matin, A., and Mukul, M. (2010) deeply study the micro-level tectonics along the course of the river Chel in the mountain area. He did not study tectonics to the lower reaches of the sedimentary surface. Still, now the river

Chel and its basin area are outside the focus of study. Few geographers maid their study in this region (Patel, P.P., 2012; Mandi, S. and Soren, K., 2016; Lama, S. and Maiti, R., 2019a; Lama, S. and Maiti, R., 2019b; Dhalia, Md K. et al., 2019). Most of their work is related to morphometry and sedimentology of Chel River. They rarely discoursed on the effects of neotectonics on Chel morphometry and sedimentology. Mandal, S., Sarkar, S. (2016) draws a correlation between neo-tectonics, morphometry, and sedimentology of the Chet basin. But, the tectonic variation of this basin area has not been identified. Tectonic variation causes different geomorphic problems of land use. The main aim of this study is to identify the tectonic variation in different parts of the study area. To satisfy this aim, the measurement and analysis of relief, basin and drainage morphometry and the primary observation and analysis of tectonic terraces and physical properties of the sedimentary facies of this area are considered the objectives of this study.

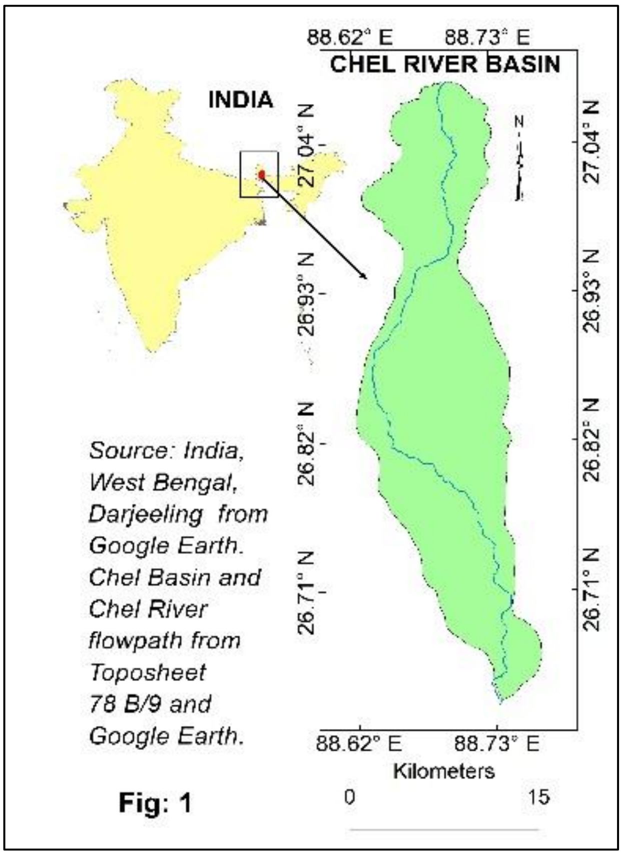

Fig: 1- Location map;

2. ABOUT THE STUDY AREA

The river Chel is a south-flowing perennial river of the mountain of eastern Himalayas. The monsoon climate is responsible for its perennial condition. It runs about 66.7 km from Darjeeling Himalayas in the north to Tista River in the south and has 388.65 sq. km basin area approximately and bounded by 27° 5'5.67"N to 26°37'42.95"N and 88°37'12.13"E to 88°45'59.06"E (Fig: 1). The river basin comprises both the mountain area of Kalimpong district and foothills plain land of Jalpaiguri district. During the rainy season, the river deposits profuse sediments to the foothills and forms the foothill plain. The mountainous terrain is the source of sediments. Different primary processes, ie. Rock-gravity processes, sediment-gravity processes, fluid-gravity processes, yield sediments. With monsoon, neo-tectonics control the process of sediment erosion and deposition. Different tectonic thrusts, ie. MCT (Main Central Thrust), RT (Ramgarh Thrust), MBT (Main Boundary Thrust), MFT (Main Frontal Thrust) are the chief inscription of tectonics. The Chel basin comprises a different type of geomorphic surface, ie. mountains, alluvial fan, river terrace and flood plain (Fig:9). Neo-tectonics are responsible for the segmentation of geomorphic surfaces. The river terrace, incision of river, meandering, escarpment, reverse graded facies profile, a repeat of coarse and fine texture in the facies sediments, are the imprints of tectonics on Chel basin.

2.1. Tectonic Setting: The eastern Himalaya is combination of Trans Himalaya (TH) and Darjeeling-Sikkim-Himalaya (DSH). MCT is the northern limit of DSH and split into MCT-1 and MCT-2 (Fig: 2) due to duplex formation in DSH (Mitra, G. et al., 2010; Mukul, M. et al. 2014). South of MCT, the MBT and MFT are formed (Yin, A. 2006). In Chel basin, the RT is formed between MCT2 and MBT (Mitra, G. et al. 2010; Mukul, M. et al. 2014). The Ghish Transverse Fault (GTF) is licated in the west of basin margin (Fig:2). Four lineaments such as the Tista lineament, Gangtok lineament, Goalpara lineament, and Kanchenjunga lineament (Fig:2) traverse the DSH duplex (Mukul, M. et al. 2014). In the north of Chel basin, the earthquake epicentres are clustered in LHD (Lower Himalayan Duplex) of Sikkim Himalaya between MCT and MBT (Mukul, M. et al.; 2014; Fig:2). In the south of LHD, the MBT (Fig:2) tectonically is less effective than MCT. The tectonically inactive MBT presently is getting active by folding of younger footwall along South Kalijhora Thrust (SKT) (Mukul, M. et al. 2014).

Mukul, M.; et all. (2014) identify Garubathan recess in the Darjeeling Himalaya (Fig: 2). This recess was folded by the GTF in the study area (Mukul, M.; et al. 2014). In this recess, the MCT-1 is identified as MT (Yin, A. 2006; Srivastava, V. et al., 2017). The RT (Pearson, O. N., and DeCelles, P. G., 2005) is recognized regionally or locally in a different name i.e. North Kalijhora Thrust (NKT) (Mitra, G. et al. 2010), Garubathan thrust (GT), Matialli Fault, Thalijhora-Jiti fault. RT (Matin and Mukul, 2010) is also comparable to MBT (Nakata, T.,1989) in the study area. Approximately 10 km south of Matialli Fault the Chalsa scarp (Mohapatra, S. R. et al. 2012) is the regional identification of MBT (Srivastava, V., 2017) and attribute to the MFT (Nakata, T., 1989). To the southern edge of Garubathan recess, the MFT/HFT locally is recognized as Baradighi Fault (Mohapatra, S. R. et al., 2012).

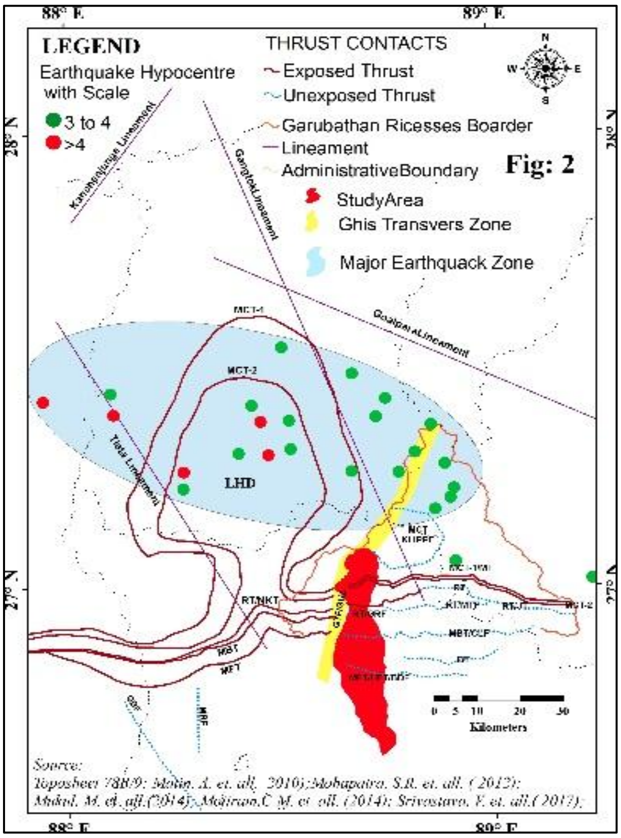

Fig: 2- Regional tectonic setting;

2.2. Geological Setting: The stratigraphy of the Darjeeling – Sikkim Himalaya (Ray, S., 1947; Ghosh, A. M. N. 1956; Acharyya, S. K., 1971; Ray, S. K., 1976; Acharyya, S. K. and Ray, K. K., 1977; Raina, V. K. 1976; Gangopadhyay, P. K. and Ray, S., 1980; Mukul, M., 2000; Bhattacharyya, K. and Mitra, G., 2009, Mitra, G. et al., 2010) also complex. The geology of the Chel Basin is structured by different tectonic thrust contacts such as MCT-1, MCT-2, RT, MBT, and MFT (Fig:2). The geological formations consist of only the lithotype of rocks. The MCT-1 thrust sheet contains Precambrian Proterozoic Darjilling Gneiss and the MCT-2 thrust sheet contains the Paro Group of rock. The RT comprises different formations i.e., Precambrian Daling group of Garubathan formation, Paleozoic Upper Permian Gondwana group of Damuda Formation, Pleistocene Formation of an old quaternary boulder bed, the MBT thrust sheet is composed of Quaternary deposits of Jalpaiguri Formation, and the younger Quaternary deposits of Duars formation (Matialy member) (Fig:3). Both the MFT thrust sheet (the hanging wall) and the footwall show a litho-geological structure of younger Quaternary deposits of Duars formation of the Matialy member group. All these lithotypes of geological formations are sequenced in two different types of sheets on the east and west sides of Chel River (Table:1). In the east, the Damuda Formation and Jalpaiguri Formation are absent and in the west the Old Pleistocene Quarternary Boulder Bed is absent. South of MCT the Reyang Formation and Buxa Formation are un-exposed and are covered under the Garubathan formation.

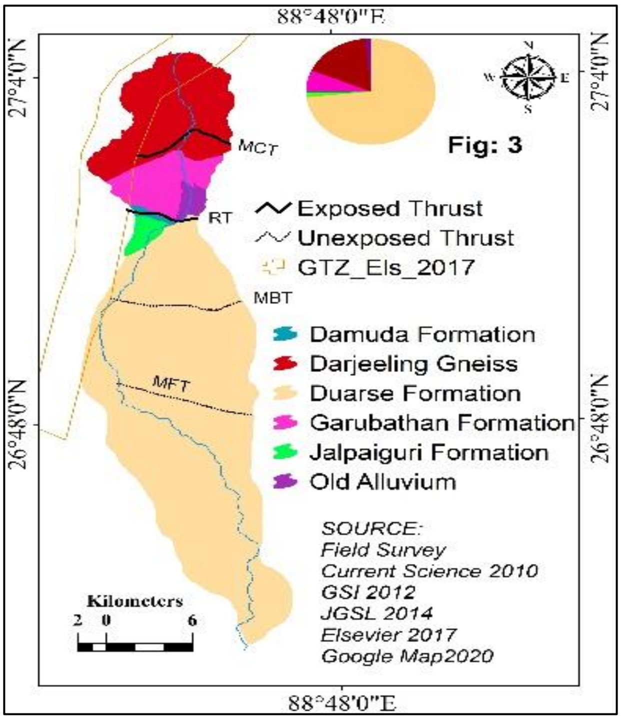

Fig: 3- Geology of the Chel basin;

<u>Darjeeling Gneiss</u> is composed of biotite-muscovite gneiss and migmatitcquartz-biotite gneiss and forms a bedding plane at an angle of about 29° toward the north (Mohapatra, S. R. et al., 2012). Sometimes the bedding plains are impossible to identify. A strong gneissic foliation is found here. For this reason, the gneisses are pronto erosion. The foliation dip direction varies from NE to NW. The *<u>Paro Group of Rocks</u>* contains Ligntse Gneiss, Augen gneiss, Prophyritic granite gneiss. Like MCT-1 these rocks are also tectonically foliated and the foliations are mostly parallel to the Daling formation of the Ramgarh thrust sheet. *<u>Garubathan Formation</u>* of the Deling group of rocks of the lower LHS (Mukul, M., 2000) is best exposed around Daling Front in Darjeeling Himalaya (Ray, S. K., 1976). It consists of phyllite, mylonitised phyllite, deformed phyllite, quartz-chlorite-biotite schist, gneiss (Mohapatra, S. R. et al., 2012).

Table:1 (Geological Succession of Garubathan Surface)

<table>
<tr><th colspan="5">Geologic Time</th><th rowspan="2">Stratigraphic Unit</th><th colspan="2">Rock Formation</th><th rowspan="2">Geomorphic Units</th></tr>
<tr><th>Division</th><th>Eon</th><th>Era</th><th>Period</th><th>Epoch</th><th>West of Chel river</th><th>East of Chel river</th></tr>
<tr><td rowspan="7">Precambrian</td><td rowspan="7">Proterozoic</td><td rowspan="7" colspan="3"></td><td>Darjeeling Gneiss</td><td colspan="2">Two-mica migmatitic gneiss</td><td rowspan="3">Greater Himalaya</td></tr>
<tr><td></td><td colspan="2">MCT-1</td></tr>
<tr><td>Paro Group</td><td colspan="2">Ligntse Gneiss, Augen gneiss, Prophyritic granite gneiss</td></tr>
<tr><td colspan="4">MCT-2</td></tr>
<tr><td rowspan="3">Daling group</td><td colspan="2">Garubathan Formation</td><td rowspan="3">Lesser Himalaya</td></tr>
<tr><td colspan="2">Un-exposed Reyang Formation</td></tr>
<tr><td colspan="2">Un-exposed Buxa Formation</td></tr>
<tr><td rowspan="8">Postcambrian</td><td rowspan="8">Phanerozoic</td><td rowspan="2">Cenozoic (Alpine)</td><td rowspan="2">Quarternary</td><td rowspan="2">Pleistocene</td><td>Indo-Gangetic Alluvial deposits</td><td>Absent</td><td>Old Boulder Bed</td><td>Himalayan foreland basin</td></tr>
<tr><td colspan="4">RT</td></tr>
<tr><td>Paleozoic</td><td>Upper Permian</td><td>Cisuralian – Guadalupian</td><td>Gondwana group</td><td>Damuda Formation</td><td>Absent</td><td>Lesser Himalaya</td></tr>
<tr><td rowspan="5">Cenozoic (Alpine)</td><td rowspan="5">Quarternary</td><td rowspan="5">Pleistocene</td><td rowspan="5">Indo-Gangetic Alluvial deposits</td><td>Jalpaiguri Formation</td><td>Duars Formation</td><td rowspan="5">Himalayan foreland basin</td></tr>
<tr><td colspan="2">MBT</td></tr>
<tr><td colspan="2">Duars Formation</td></tr>
<tr><td colspan="2">MFT</td></tr>
<tr><td colspan="2">Duars Formation</td></tr>
</table>

Source: After Matin, A., and Mukul, M., 2010; Mohapatra, S. R. et. al., 2012, Field Survey

The Phyllites are sometimes become intercalated with Quartzite bands (Matin, A. and Mukul, M., 2010). The Daling Phyllite thrust over Pleistocene boulder gravel beds in the east of Chel river and thrust over Damuda formation in the west of Chel river (Fig:3). *Damuda formation* of the Gondwana group is consisting medium to coarse grain pebbly sandstone. Alternative layers of sandstone and shale are found here. The coal streaks and lensoid carbonaceous shale are the remarkable characteristics of this part. The *Pleistocene Formation* of the old Quaternary Matali Member Group comprises a quaternary bolder bed is overlaying the Darjeeling gneiss and Phyllite layer. In some pleases the phyllite layer has been exposed to the surface. *Jalpaiguri formation* of Pleistocene age consists of sand, pebble, cobble and boulder beds. It is a semi-consolidated Quaternary alluvial deposit on the west bank of Chel river. The alternative layer of gritty sand and boulder beds are a common occurrence here. Their sandy beds are mostly horizontal, which indicates the fluvial depositional environment rather than the tectonic environment. *Duars Formation* of younger Quaternary Matali Member have a thrust contact with Old Boulder Bed of Quarternary Pleistocene Formation on the east bank of Chel River along Dudh Khola sections and has a thrust contact with Jalpaiguri Formation on the west bank of Chel Rive (Mohapatra, S. R. et al., 2012). It is composed of unconsolidated pebbles, cobbles, and boulders in a brown-coloured highly oxidized sandy soil with the weathered horizon and capped by red soil.

The Siwalik section is absent in this recess because the recess has led to a new transverse structure of GTZ at a high angle. The Ghish River presently flows through this transverse zone at the mountain front. The mountain front in the western part of this transverse fault is characterised by the Quaternary Siwalik deposit, whereas in the eastern part of a transverse fault the mountain front is defined by a thrust of Proterozoic Daling Formation of rock on Gondwana rocks. There are blind imbrications in the south of mountain fronts that form E-W trending fault scarp. From north to south,

International Research Journal of Engineering and Technology (IRJET) e-ISSN: 2395-0056
Volume: 09 Issue: 06 | June 2022 www.irjet.net p-ISSN: 2395-0072

these scarps are arranged as MCT-1, MCT-2, RT, MBT, BT, and MFT (Fig:2).

To the south of MBT (Nakata, T.,1989) or RT (Matin and Mukul, 2010) the Siwalik belt is partly missing between the Chel and Pana Rivers where the Himalayan front retreats several kilometres north following N–S directed fault lines along the rivers Chel (Starkel, L., Sarkar, S., Soja, R. and Prokop, P., 2008; Mukul, M. et al., 2008; Mukul, M., 2010). Here the Siwalik belt is replaced by quarternary bolder and recent alluvium deposits.

Table: 2 (Morphometric Techniques)

Technique	Description	Source
	Relief Aspects	
Absolute Relief	Height from mean sea level	Pareta , 2011
Relative Relief	Height from local base level	Hamnowd 1954 and Thaver 1955
Dissection Index	Relative Relief / Absolute Relief	De Smet (1951)
Average Slope	tanθ = (C×I)/Wc. When: C = Average No of Contour crossing per unit area, I = Contour interval, Wc = 636.6 (Wentworth's Constant)	Wentworth (1930)
Ruggedness Index	Ruggedness Index = (Mean Relief-Minimum Relief)/ (Maximum Relief -Minimum Relief).	Strahler (1964)
	Primary Basin Properties	
Area (sq. km) (Ab)	---	SRTM DEM
Perimeter (km) (Pb)	---	SRTM DEM
Length (km) (Lb)	---	SRTM DEM
Width (km) (Wb)	---	SRTM DEM
	Linear and Areal Aspects of Basin	
Basin Shape Factor (BSF)	Lb / Wb	Morisawa, 1958
Basin Eccentricity (Eb)	(Lcm2 – Wcm2)0.5/Wcm; Lcm=straight length of sub-basin from the centre to mouth, Wcm=Width of sub-basin at the centre of mass and perpendicular of Lcm	Black, 1972
Elongation Ratio (Re)	The ratio of a diameter (2r) of a circle of the same area of a basin to the maximum length (Lb) of that basin	Schumm's, 1956
Lemniscate's value (K)	Lb /4Ab)/	Chorley, 1957
Form Factor (Rf)	Ab/Lb	Horton, 1932
	Basin Area & Basin Perimeter Co-Relation	
Circularity Ratio (Rc)	Ab/Ac; Ac= circle that bears the same perimeter of the basin	Miller, 1953; Strahler, 1964
Relative perimeter (Pr)	Actual basin area (Ab)/the actual basin perimeter	Schumm, 1956
Compactness Co-efficient (Cc)	Pb/√2πAb; Basin area=Ab and basin perimeter = Pb	Horton, 1932
Gravelius's shape index (Kg)	Pb/√(2&πAb); Basin area=Ab and Basin perimeter = Pb	Musy, 2001
	Linear Aspects of the Stream Network	
Stream Order (U)	----	Strahler ,1952
Stream Number (Nu)	Total count of order u	Horton, 1945
Stream Length (Lu)	Total length of order u	Strahler ,1964
Mean Stream Length (Lū)	Nu/Lu	Strahler ,1964
Stream Length Ratio (RLu)	$Lu_n/(Lu_{n-1})$	Horton, 1945
Mean Stream Length Ratio (RLū)	$L\bar{u}_n/L\bar{u}_{n-1}$	Horton,1945; Dingman, 2009
Bifurcation Ratio (Rb)	Nu_n/Nu_{n+1}	Schumm,1956, Dingman, 2009

Rho Co-efficient (Rc)	RLū / Rb	Horton, 1945
Areal Aspects of the Stream Network		
Drainage Texture (Dt)	∑Nu /Pb	Horton, 1945
Texture Ratio (Rt)	∑N1/ Pb	Schumm, 1956
Stream Frequency (Fs)	Total number of streams per unit area (sq km)	Horton,1932, 1945
Drainage Density (Dd)	Length of drainage per unit area (sq km)	Horton, 1932
Infiltration Number (If)	Fs*Dd	Smith,1950; Faniran,1968
Drainage Intensity (Di)	Fs/Dd	Faniran, 1968
Wandering Ratio (Rw)	Lu/Lb	Surkan, 1967
Fitness Ratio (Rf)	Lu/Pb	Melton, 1957
Channel Morphometry		
Actual Channel Length (km) (Cl)	---	SRTM DEM
Aerial Channel Length (km) (Acl)	---	SRTM DEM
Actual Valley Length (km) (Vl)	---	SRTM DEM
Arial Valley Length (km) (Avl)	---	SRTM DEM
Sinuosity Index (Si)	Cl/Vl	Miller, 1968
Channel Index (Ci)	Cl/Acl	Miller, 1968
Valley Index (Vi)	Vl/Avl	Miller, 1968
Standard Sinuosity Index (Ssi)	Ci/Vi	Mueller, 1968
Hydraulic Sinuosity Index (Hsi)	(Ci-Vi)/(Ci-1) *100	Mueller, 1968
Topographic Sinuosity Index (Tsi)	(Vi-1)/Ci-1) *100	Mueller, 1968

3. MATERIALS AND METHODS

The variation of geology, relief, morphometry and sedimentology is the result of neotectonic variation of the Chel basin. So the neotectonic variation of this basin is identified based on relief, morphometry and physical characteristics of sediment. The primary concept of geology and neotectonic of the study area is studied from different types of literature. In the field, various dimensions of geology, neotectonics and morphometry of terrain and drainage are identified, measured and perceived with the help of GPS (Garmin 550), compass, clinometer. To perceive the neotectonic intensity only the geomorphic characteristics of the river terrace and physical properties like texture, the structure of sedimentary facies are primarily observed in the field. This study is performed mainly based on relief and drainage morphometry, which is extracted and analyzed from SRTM DEM data and topo sheet 78B/9 of the survey of India with the help of GIS Software (Arc GIS, Map info and Quantum GIS) and Microsoft excel. Google Earth image is used to delineate the study area. Different parameters like height, area and length (Table: 2) are considered to measure the morphometry of the basin.

4. RESULTS AND OBSERVATION

4.1. Aspects of Relief

According to Smith, G.H. (1935), "relief is a concept intended to describe the vertical extent of landscape feature, without reference to absolute altitude or slopes," The long profiles L1 and L2 (Fig: 4c) show a prominent break in slope at each thrust contact i.e., MCT, RT, MBT, and MFT. Based on break in slope the Chel basin is sub-divided into five zones i.e. - the mountain, upper fan, middle fan, lower fan and flood plain area (Fig: 3), which ranges between 800.1m to 2500m, 300.1m to 800m, 200.1m to 300m, 120.1m to 200m, 80m to 120m (Fig: 4a) and are identified as tectonic zone one (I), two (II), three (III), four (IV) and five (V), respectively. The respective class widths of these relief zones are about 1700m, 500m, 100m, 80m, and 40m. The mean and mean deviation of the classes of the north surface of RT is 1100m and 600m respectively. Whereas, they become 73.33 m and 22.22m respectively in the southern part of RT.

There is a remarkable height difference between the upper fan and middle fan, which are separated by the RT. The upper fan is about 300m-400m higher than the middle fan surface. The upper fan is known as the Garubathan surface and the remaining southern surface is known as the Rangamati surface. The cross profiles C1 to C5 (Fig: 4b) present a highly undulating surface in the north of RT and a very levelled and rough surface in the south of RT. In the mountain area, the MCT is restricted by GTZ to its western edge (Fig: 2). Here the northern margin of the second zone crosses the MCT due to headward erosion of the river. But the MCT reduce headward erosion near GTZ. In the foothill plain, the MFT diagonally crosses the margin of the fourth and fifth relief zone in the northwest to southeast direction. The fourth relief zone of the Chel basin has been tilted up to its western side and as a result, its southern edge extends southward beyond MFT. Like the fourth relief zone, the third zone also extends southward beyond MBT. But here the southern margin of this third zone is almost parallel with this thrust contact. The cross profile C3 shows an eastward elevated surface and the field observation also reveals the headward erosion at this place of the third zone.

The *relative relief* represents an index of the stage of development (Partsch, 1911) and the ratio between relative and absolute relief reveals the “dynamic potential” of the area (DovNir, 1957). Both the stage of development and “dynamic potential” is important to understand the neotectonic variation of the area. The relative relief of the area ranges between 480 m to 65 m and 65 m to 4 m in the northern and southern part of RT respectively (Fig: 5). Remarkably the highest value of relative relief zone of 345m to 480m is found near GTZ rather than MCT. Near RT and MBT, a patch of the second-lowest relative relief zone of 20 m to 65 m is observed.

De Smet (1951) first used *dissection index* to explain the erosional condition of a surface, which depicts the dimension of erosion (Dubey, 1986), stage of development of a landscape (Singh & Dubey, 1994), basin dynamics and the stage of stream development (Nir 1957, Mukhopadhyay 1973, Barman, 1986). The dissection index value is ranged between 0 and 1 (Davis, 1905) that stands for absence and maximum erosion, respectively (Rai et al., 2017a & 2017b; Rai et al., 2018). A high erosive nature of the centripetal tributaries of Chel River highly segmented the RT, which records the highest dissection index value (0.26-0.60) of the basin for its tectonic instability. However, the MCT sheet is showing a moderate to very low dissection index of 0.03 to 0.26. All the surfaces in the south of RT dominate a very low value (0.03-0.10) of dissection index. But some pockets (Fig: 6) of this surface near MBT and MFT are dominated by moderate to a low value (0.10-0.26) of dissection index.

Active neotectonics control slope processes (Jaboyedoff, et al., 2011). Five respective *zones of slope* (Fig: 7) are observed. In the south of RT, the alluvial surface is showing the slope of 1°-7°. However, at the middle-eastern part of this alluvial surface along with MBT, a patch of the area shows steep slopes which are aligned in a north-south direction and ranged between 7°-17°. Near MCT, two little and elongated patches of this slope zone are oriented in a north-south direction on RT sheet (Fig:7) in the eastern bank of Chel river, where moderate (17°-25°) to high (25°-35°) steepness is the general characteristics of this area. The field observation identifies this surface is a river terrace. MCT sheet showing the maximum steepness of 25°-65°.

Strahler (1964) calculated the *ruggedness index* that is closely related to different morphometric characteristics i.e., slope, dissection index, and drainage texture and drainage density of geomorphic surface (Hook 1955, Mukhopadhyay 1973, 1977, 1978a, 1978b and 1979c). A high value of ruggedness index not only depends upon slope steepness but also depends upon the length of the steep slope. However, the slope is the function of neotectonic instability (Jaboyedoff, et al., 2011). *Ruggedness Index* is uniform (Fig: 8) throughout the basin area and ranges between 0.3-0.7. But a little patch of low value ranging between 0.7-0.9 is observed in the eastern part of MBT.

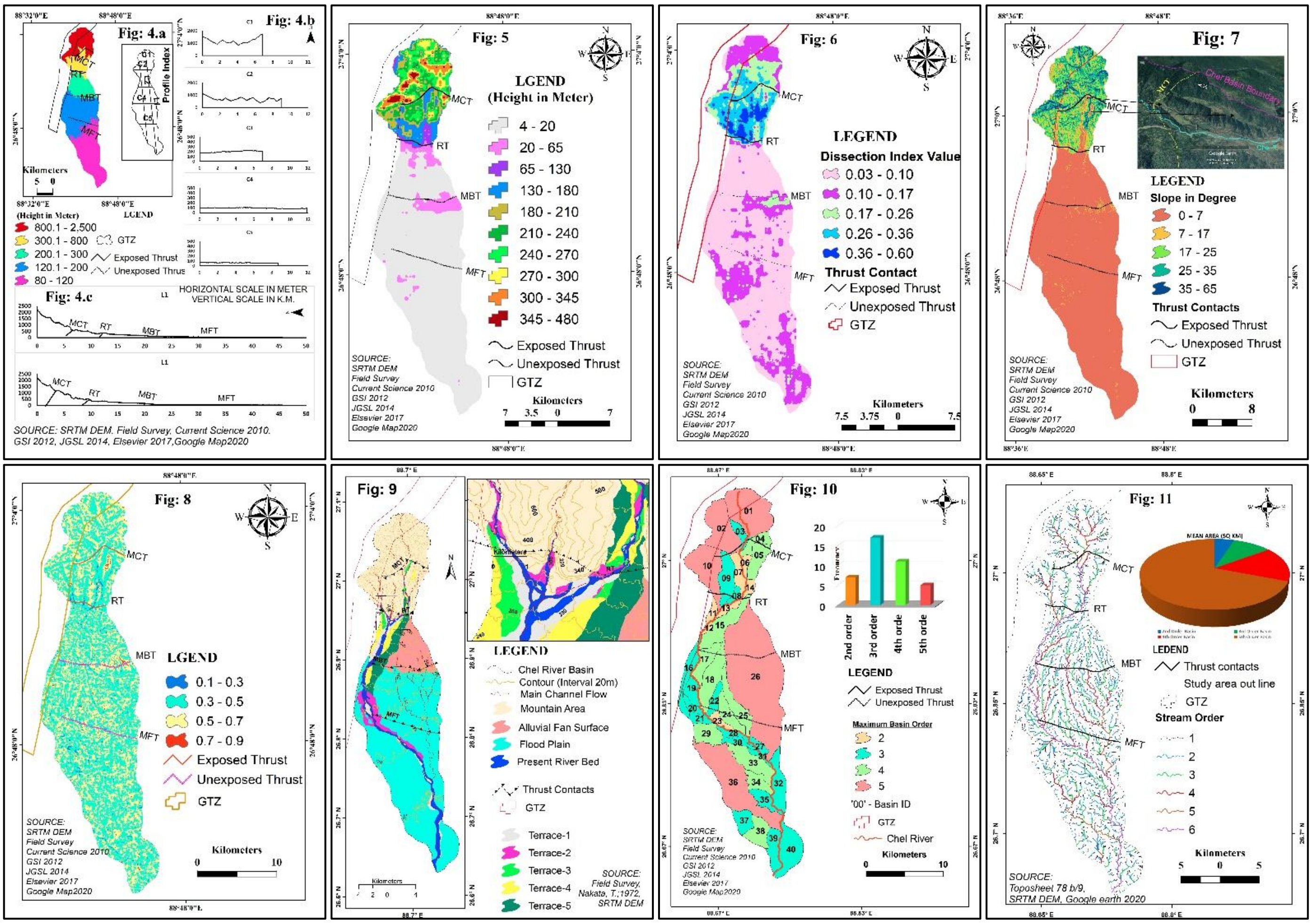

Fig: 4- Relief map; **Fig: 5-** Relative relief map; **Fig: 6-** Dissection index map; **Fig: 7-** Slope map; **Fig: 8-** Ruggedness index map; **Fig: 9-** Geomorphic surface and river terrace of the study area; **Fig: 10-** Flow direction map; **Fig: 11-** Order wise sub-basins of the study area; Fig: 12- Stream order of the study area.

4.2. Aspects of Drainage Basin

Based on relief and drainage, the Chel basin has been divided into forty sub-basin (Fig: 10), which represents a sub-system within a major system of the stream network. All the sub-basins except No 26 are accommodated within thrust contacts in the study area. Four types of sub-basin i.e., 2nd, 3rd, 4th and 5th order are identified in the study area (Fig: 10). The order wise frequency of the sub-basin is 7, 17, 11 and 5 respectively.

In the tectonic zone I, II, III, IV and V the respective frequencies of the 5th order basin are 2, 1, 0, 0, 1; 4th order basins are 0, 2, 1, 4, 4, 3rd order basin are 1, 2, 0, 3, 11 and the 2nd order basin are 0, 3, 3, 0, 1. The 4th, 3rd and 2nd order basins cover about 8.56 sq. km, 5.29 sq. km and 2.68 sq. km mean area, respectively. The 5th order sub-basin covers about 20.80 sq. km mean area in the mountain surface and 85.19 sq. km mean area in the fan surface. Remarkable that, in the

Table: 3 (Aspects of Drainage Basin)

Sub-basin Properties		North of MCT		MCT-RT		RT-MBT		MBT-MFT		South of MFT	
		Total	Mean	Total	Mean	Total	Mean	Total	Mean	Total	Mean
Horizontal Properties											
Area (sq. km)	(Ab)	47.19	15.73	48.04	6.86	18.93	4.73	46.65	7.77	130.14	7.66
Perimeter (km)	(Pb)	52.51	17.5	91.34	13.05	51.3	12.82	109.7	18.29	253.47	14.91

								4			
Length (km)	(Lb)	19.04	6.35	37.45	5.35	21.91	5.48	47.92	7.99	96.66	5.69
Width (km)	(Wb)	12.21	4.07	14.39	2.06	5.55	1.39	11.31	1.89	36.54	2.15
Length from centre to mouth (km)	(Lcm)	9.42	3.14	22.08	3.15	10.74	2.69	23.1	3.85	50.06	2.94
Width from centre and perpendicular to length (km)	(Wcm)	4.3	1.43	5.72	0.82	2.11	0.53	3.9	0.65	16.37	0.96
Length & width Co-relation											
Basin Shape Factor	(BSF)	6.47	2.16	19.18	2.74	17.26	4.31	27.14	4.52	52.18	3.07
Basin Eccentricity	Eb (τ)	7.57	2.52	28.18	4.03	19.11	4.78	35.19	5.86	67.54	3.97
Length & Area Co-relation											
Diameter of the circle that bears the same area of the basin (m)	(2r)	12656	4218.7	19096	2728	8813	2203	18524	3087	48406	2847.4
Elongation Ratio	(Re)	1.93	0.64	3.64	0.52	1.61	0.40	2.5	0.42	9.26	0.54
Lemniscate's value	(K)	2.91	0.97	8.54	1.22	8.12	2.03	13	2.17	23.09	1.36
Form Factor	(Rf)	1.04	0.35	1.5	0.21	0.52	0.13	0.86	0.14	4.43	0.26
Area & Perimeter Co-relation											
Area of the circle that bears the same perimeter of the basin (sq. km)	(Ac)	77.92	25.97	111.10	15.87	64.80	16.20	173.76	28.96	397.91	23.41
Circularity Ratio	(Rc)	1.65	0.55	3.07	0.44	1.22	0.31	1.91	0.32	6.76	0.4
Relative perimeter	(pr)	2432.1	810.7	3153	450.4	1197	299.3	2529.4	421.6	7461.5	438.91
Compactness Co-efficient	(Cc)	5.89	1.96	15.07	2.15	10.38	2.6	15.75	2.62	39.62	2.33
Gravelius's shape index	(Kg)	8.33	2.78	21.32	3.05	14.68	3.67	22.27	3.71	56.03	3.3

0.00-Heighest value, 0.00-Lowest value

south of RT, most of the 3rd and 4th order sub-basins are arranged in the western and eastern bank of the river Chel, which are highly elongated. Alternatively, in the mountain surface in the north of MCT, the 5th order sub-basins (No-1, 2) are circular and between MCT and RT six small (6.86 sq. km mean area) sub-basins (No-5, 6, 7, 8, 9 and 14) with their maximum order of 2 to 4 are developed. In this region, only one 5th order sub-basin (No: 10) is located over GTZ.

The *Ab, Pb, Lb, Wb, Lcm, Wcm* (Table: 3) are the basic linear properties of the sub-basins. *Ab, Wb* and *Wcm* show their maximum mean values in the north of MCT, whereas the maximum mean values of *Pb, Lb* and *Lcm* are recorded between MBT and MFT. Except for *Lb,* all other minimum values are recorded in the RT-MBT zone and the zone of MCT-RT records the minimum *Lb* value. Neotectonic is a facto of co-relation between basin properties. To understand the co-relation between *Length, width & Area* the *BSF, Eb, Re, K* and *Rf* and between *Area & Perimeter* the *Rc, Pr, Cc* and *Kg* of sub-basins are calculated in the different tectonic zone of the study area (Table: 3). Neotectonics controlled all these properties that depict the shape and slope conditions of the Chel basin.

Elongated sub-basins are tectonically active (Lari, A. A. et al.; 2016). Cease of tectonic upliftment gradually forms the sub-basin in a circular shape (Burbank, D.W. and Anderson, R.S. (2001). The range of *Re* values from 0 to 1 is grouped into <0.7, 0.7-0.8, 0.8-0.9 and >0.9, which refers to elongated, less elongated, oval and circular basin shapes, respectively (Strahler, 1964). This value is related to relief and slope (Molin et al. 2004). The value of 1 is associated with low relief and the value from 0.6 to 0.8 is observed in the high relief zone (Strahler, 1964). In the north of MCT, in mountain area, sub-basin 1, 2 and 10 are showing 0.83, 0.68 and 0.55 *Re* values, which are oval and elongated shape respectively (Table:3) and between MCT and RT the range of *Re* value from 2.14 to 4.9 present the highly elongated sub-basins. In the south of RT, instead of low relief (80 m to 300 m) and low slope (0° to 7°), the mean *Re* values between 0.2 and 0.5 represent the elongated sub-basin. Field survey reveals that these sub-basins are developed on the tectonic terraces that are aligned in a north-south direction implies the impact of GTZ. The value of *K,* which depicts slope conditions (Chorely, 1957), is directly proportional to the elongated shape of a basin. The range of *Rf* value becomes 0 to 1, which indicates an elongated (*Rf*=0) and circular (*Rf*=1) basin shape (Rai, P. K. et al.; 2019). Lower the *BSF* value indicates higher circularity and stable tectonic conditions. The BSF values >4, 4-3 and <3 refers to tectonically active, semi-active and inactive conditions (Hamdouni, R. et al., 2007). Tectonic zone one shows the maximum mean value of *Re* and *Rf*, and the minimum mean value of *BSF, Eb* and *K*. The RT-MBT zone records the minimum mean value of *Re* and *Rf*. Zone MBT-MFT records maximum mean *BSF*, *Eb* and *K* value (Table: 3).

The *Rc* value varies from 0 to 1 and is directly related to the basin circularity (Miller, 1953). In the study area, this value is recorded between 0.17 and 0.73. Out of forty sub-basins twenty-two (above 50%) sub-basin records *Rc* value from 0.1 to 0.39, ten sub-basins record the value between 0.40 and 0.50, six sub-basins record the value between 0.50 and 0.58 and only two basins record the value above 0.70 (Table: 3). All these phenomena support the elongated nature of most of the sub-basin. Overall, above 70% sub-basin (No-32) appear as highly elongated (Rc <0.50). The mean value of *Pr* gradually increases from MCT to MFT and after MFT, the value again increases in the south (Table:3). *Cc* is an indicator of slope (Rai et al., 2017a & 2017b; Rai et al., 2018), which gradually increases from north to south with the decreasing of slope. Like the circularity ratio, the *Kg* value also announces the elongated nature of the sub-basins. The increasing value also mentions the increasing nature of elongation of the sub-basins.

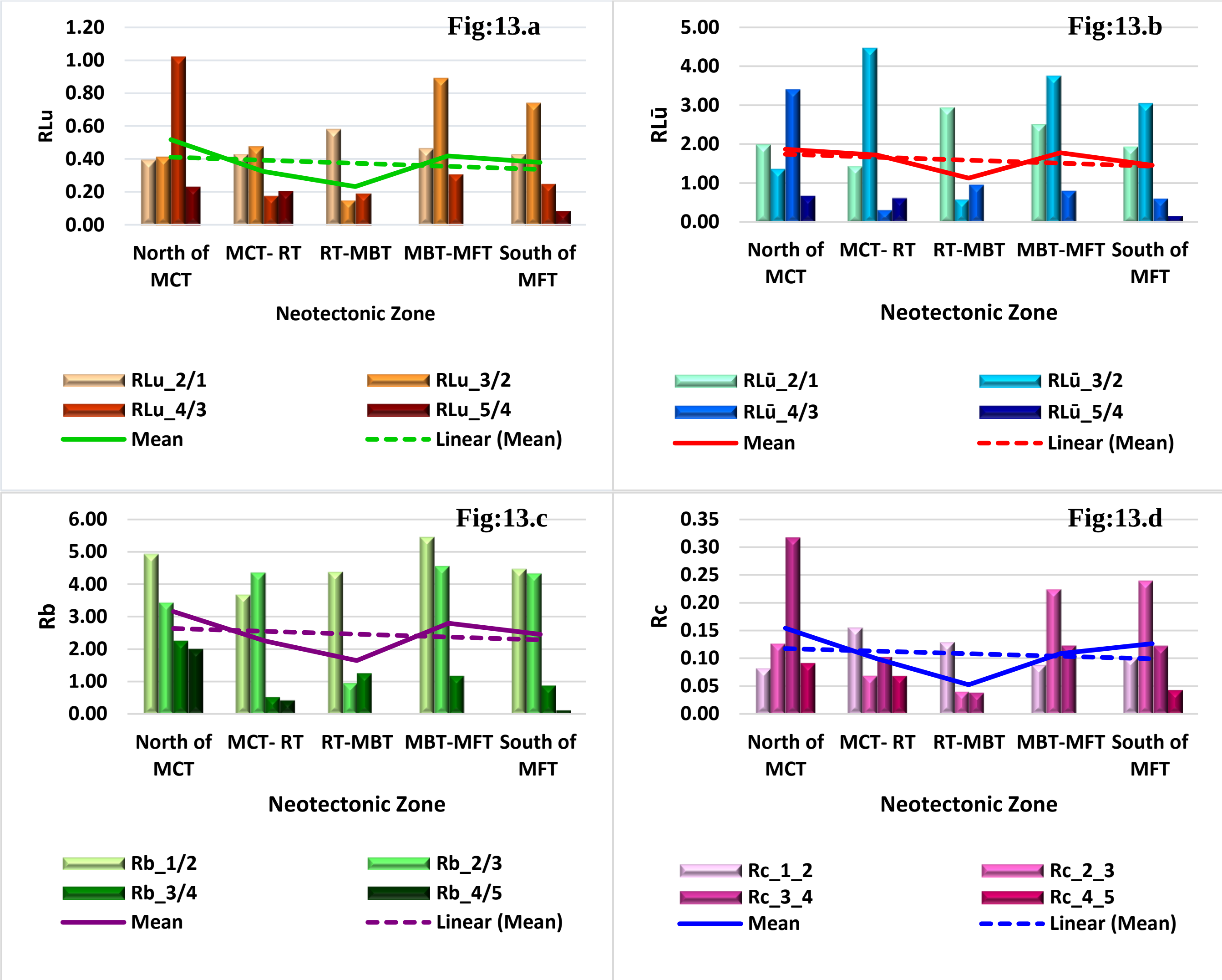

Fig:13.a: Distribution of Rlu in the different tectonic zone, **Fig: 13.b:** Distribution of RLū in the different tectonic zone, **Fig: 13.a:** Distribution of Rb in the different tectonic zone, **Fig: 13.a:** Distribution of Rc in the different tectonic zone.

4.3. Aspects of Stream Network

Stream networks, which transport eroded material of basin surface from upslope to downslope, are linear properties of a drainage basin. *U*, *Nu* and *Lu* are the basic components, which directly or indirectly depict the tectonic variation of the surface under study. The main river Chel attains the highest order *(U)* of 6 near MCT (Fig: 11).

Table: 4 (Aspects of Stream Network)

	Stream Properties	North of MCT		MCT-RT		RT-MBT		MBT-MFT		South of MFT	
		Sum	Mean	Sum	Mean	Sum	Mean	Sum	Mean	Sum	Mean
	Linear Aspects										
Order 1	Frequency (Nu1)	312	104	321	46	104	26	273	46	855	50
	Length in km (Lu1)	86.8	28.93	83.75	11.96	36	9	79.83	13.3	237.45	13.97
	Mean Length in km (Lū1)	0.28	0.28	0.26	0.26	0.35	0.35	0.29	0.29	0.28	0.28
Order 2	Frequency (Nu2)	72	24	91	13	25	6	52	9	198	12
	Length in km (Lu2)	32.27	10.76	34.13	4.88	19.59	4.81	38.12	6.35	106.45	6.26
	Mean Length in km (Lū2)	0.45	0.45	0.38	0.38	0.78	0.78	0.73	0.73	0.54	0.54
Orde r 3	Frequency (Nu3)	20	7	9	1.10	5	1	11	2	43	3
	Length in km (Lu3)	10.84	3.61	16.38	2.34	7.33	1.83	27.64	4.61	52.08	3.06

	Mean Length in km (Lū3)	0.54	0.54	1.82	1.82	1.47	1.47	2.51	2.51	1.21	1.21
Order 4	Frequency (Nu4)	6	2	4	1	1	0	3	1	7	0
	Length in km (Lu4)	14.94	4.98	5.51	0.79	5.72	1.43	10.57	1.76	14.8	0.87
	Mean Length in km (Lū4)	2.49	2.49	1.38	1.38	5.72	5.72	3.52	3.52	2.11	2.11
Order 5	Frequency (Nu5)	2	1	1	0	0	0	0	0	1	0
	Length in km (Lu5)	5.04	1.68	5.87	0.84	0	0	0	0	10.13	0.6
	Mean Length in km (Lū5)	2.52	2.52	5.87	5.87	-	-	-	-	10.13	10.13
TOTAL	Frequency (NuT)	412	137	426	61	135	34	339	57	1104	65
	Length in km (LuT)	149.9	49.97	145.64	20.81	68.64	17.16	156.16	26.03	420.92	24.76
	Mean Length in km (LūT)	0.36	0.36	0.34	0.34	0.51	0.51	0.46	0.46	0.38	0.38
Areal Aspects											
Drainage Texture (Dt) (Number/km)			6.96		4.09		1.98		3.01		3.66
Texture Ratio (Rt) (Number/km)			5.29		3.05		1.53		2.42		2.82
Stream Frequency (Fs) (Number/sq km)			8.07		9.34		6.08		7.1		8.17
Drainage Density (Dd) (km/ sq km)			2.88		3.00		3.25		3.30		3.17
Infiltration Number (If)			60.36		37.82		13.72		21.56		30.74
Drainage Intensity (Di)			0.003		0.003		0.002		0.002		0.003
Wendering Ratio (Rw)			7.32		3.33		2.44		3.29		3.96
Fitness Ratio (Rf)			2.52		1.36		1.03		1.4		1.41

0.00-Heighest value, 0.00-Lowest value

A stable environment provides the inverse relation of *Nu* and *Lu* with relief and *U*, and the direct relation of *Lū* with *U* (Horton, 1945). Climate or neotectonics distort these co-relations. In the geomorphic surface under study, the recorded minimum value of *Nu* and *Lu* of all order (*U*) in the RT-MBT zone (Table: 4) that point out the distortion of this normal co-relation. The stretching of the 26th sub-basin over the un-exposed thrust contacts of MBT and MFT (Fig: 10) argued for longtime climatic stability. This climatic stability advocate for neotectonic instability that causes such distortion of stream network in this area. In this neotectonic zone, the presence of the highest value of *Lū1* with the lowest value of *Nu1* and *Lu1* (Table: 4) signifies the development of long 1st order streams (Strahler, 1964) that accelerates the intensity of permeability and infiltration (Chitra et al., 2011). A field study reveals that a coarse texture (unsorted boulder deposits with colluvium), which is the outcome of RT neotectonics, is responsible for this type of stream network. The RT upliftment restricted the propagation of the upper fan surface and resultant the deposition of coarse gravel in this area. The absence of the 5th order stream in the low relief zone (between RT and MFT) (Table: 4) highlight the unstableness of this area.

The *RLu* is an indicator of the stage of development of any geomorphic surface (Pareta, K and Pareta, U., 2011). Gradual decreasing of *RLū* value from one order to the next order signifies the late youth stage of geomorphic development (Singh and Singh, 1997). In a geomorphic surface, the tilted steep-sloped area records higher *RLu* and *RLū* values. A remarkably lower value of *RLu* and *RLū* of RT-MBT zone than its southern low relief zone (after MBT) (Fig:13.a & 13.b) argued for rejuvenation of this area. The *Rb* is inversely related to *U* (Strahler, 1964) in a stable tectonic environment. This co-relation does not match between MCT and MBT in the study area (Fig: 13.c). Geology and lithology (Fig: 3) is responsible for this anomaly (Strahler, 1964; Chow, 1964; Verstappen, 1983; Rai et al., 2014; Singh et al., 2013). The recorded lowest *Rb* value between RT and MBT (Fig: 13.c) is the lesser effect of structural control (Strahler, 1964; Verstappen, 1983) on this area than the MCT-RT zone. The area in the north of MCT and south of MBT shows that the *Rc* is directly related to the *U* of the area, which is normal (Fig: 13.d). But the area between MCT and MBT is showing an inverse correlation (Fig: 13.d).

Dt is the expression of spacing of stream channels (Singh, 1980), which vary in *Rt* under differential lithology, infiltration capacity and relief aspect of the surface (Rai et al., 2017a & 2017b; Rai et al., 2018). Higher *Fs* refers early stage of land development or rejuvenation of an erosional surface (Singh, 1980). *Dd* defines rupturing of topography in a neotectonic environment (Ritter, D.F., et al., 1995). The *If, Di, Rw* and *Rf* help to perceive the variation of infiltration, the intensity of surface runoff, shifting nature of the stream, and topographic fitness (Rai et al., 2017a & 2017b; Rai et al., 2018), respectively, of the Chel basin under variable litho-structural control. In the study area, the concentration of the highest value of all these areal components of the stream network (Table: 4) designates the variation of active litho-structural control over surface hydrology in this tectonic zone.

4.4. Chel River Flow Path Characteristics

There is a prominent signature of neo-tectonics along the main flow path of the river Chel. The river terrace, incised channel and meandering are the imprints of tectonics impacts. A field study reveals that near MCT four river terraces and near RT five river terraces (Fig: 9) are identified in the field. The upper terrace (No-5) is composed of a clast supported gravely boulder bed. The clast size gradually decreases to its lower terraces. The lower terraces gradually become rich in a matrix. In the south of RT, the upper terraces stretch across MBT. All the terraces lose their height and marge with flood plain at their southern edge.

Length of *Cl, Acl, Vl* and *Avl* are the primary properties that determine channel sinuosity. The lower value of the sinuosity index is inversely related to tectonic stability (Jabbari, N., et al., 2012). To determine the variation of tectonic impact the main channel flow path has been divided into several segments based on the Muller (1968) concept and different indexes (Table: 5) are calculated. Sinuosity indexes of this river are recorded maximum either in the north of MCT or in the south of MFT.

Table: 5 (Aspects of Chel River Channel)

	Description	Tectonic Zone: North of MCT	MCT-RT	RT-MBT	MBT-MFT	South of MFT
Components	Actual Channel Length (km) (Cl)	8.70	9.06	9.10	8.62	31.25
	Aerial Channel Length (km) (Acl)	6.83	7.55	8.09	7.15	24.30
	Actual Valley Length (km) (Vl)	8.76	9.77	8.82	8.67	27.73
	Arial Valley Length (km) (Avl)	6.72	7.62	7.91	7.14	23.39
Co-relations	Sinuosity Index (Si)	0.99	0.93	1.03	0.99	1.13
	Channel Index (Ci)	1.27	1.20	1.12	1.20	1.29
	Valley Index (Vi)	1.30	1.28	1.12	1.22	1.19
	Standard Sinuosity Index (Ssi)	0.98	0.94	1.01	0.99	1.09
	Hydraulic Sinuosity Index (Hsi)	-11.08	-41.08	7.71	-5.19	35.23
	Topographic Sinuosity Index (Tsi)	111.08	141.08	92.29	105.19	64.77

0.00-Highest value, 0.00-Lowest value

4.5. Lithology and Physical Properties of Sediment

In the Himalayan region, a common phenomenon is that the northern thrust sheets are laying over the southern thrust sheet. But near MCT the Garubathan formation has been thrust over Darjeeling Gneiss from the south (Fig: 14.g). Near the Garubathan market at RT, the underlying scale-like foliated phyllite rock of Garubathan formation has been warp upward and its old quaternary deposit thrust over phyllite rock from the north (Fig:14.e). Frequent repetition of the clast-supported layer and the matrix-supported layers is a general character in the south of RT. The clast-supported boulders are deposited over matrix-supported sand deposits near RT (Fig: 14.h) and MBT (Fig: 14.i). The facies near RT records two boulder beds where near MBT it shows only one boulder bed. The distal part of the alluvial fan stores the fine sediments. Beyond the fan surface, in flood plain area the boulder facies (Fig: 14.f) is also observed. Based on the 'B' axis orientation of boulder clasts the fan diagrams have been constructed, that depict the duration of different directions of streamflow (Fig:14.b, 14.c & 14.d). The river Chel changes its flow direction from south-east to south-west near RT (Fig: 14.b), from south-east to south near MBT (Fig: 14.c) and from south-west to the south (Fig: 14.d) in the flood plain area.

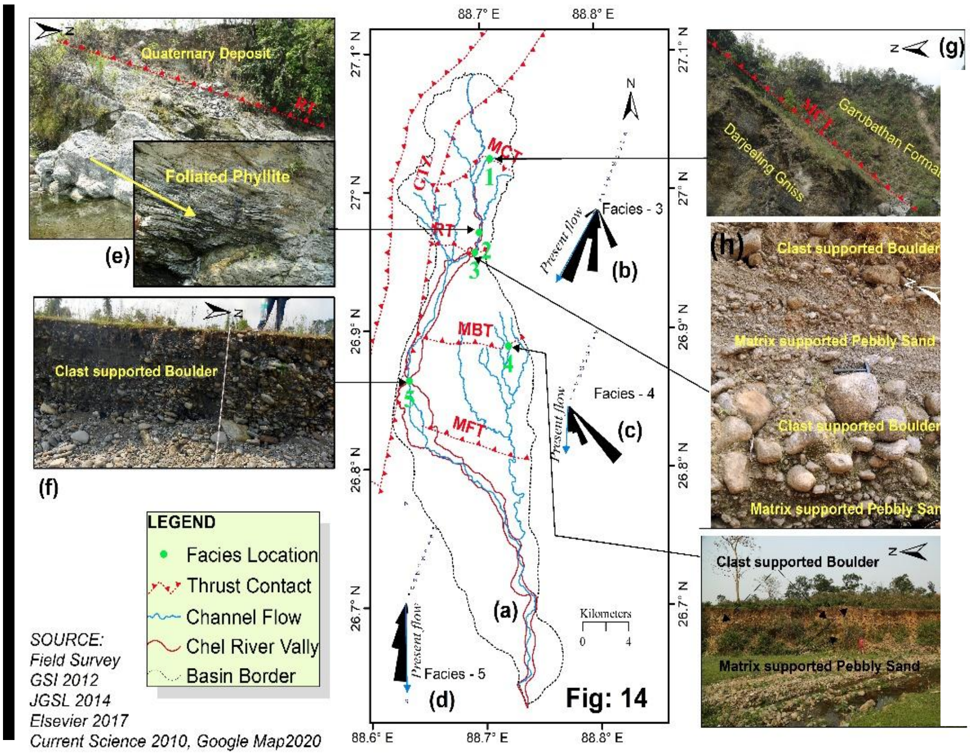

Fig-14.a: Location of facies in the different tectonic zone of the study area; **Fig-14.b:** Fan diagram of the facies No 3 that showing shifting of stream flow direction from southeast to south west; **Fig-14.c:** Fan diagram of the facies No 4 that showing shifting of stream flow direction from southeast to south; **Fig-14.d:** Fan diagram of the facies No 5 that showing shifting of stream flow direction from southwest to south; **Fig-14.e:** RT thrust contact; **Fig-14.f:** Clast supported boulder deposits; **Fig-14.g:** MCT thrust contact; **Fig-14.h:** Alteration of boulder and sand facies near RT due to neotectonic effects; **Fig-14.i:** Alteration of boulder and sand facies near MBT due to neotectonic effects

5. INTERPRETATION

5.1. Relief aspects

The impact of MCT, RT, MBT, MFT and GTZ over relief and drainage morphometry is not uniform all over the Chel basin. The parallel situation of the thrust contacts with the relief zone (Fig: 4.a) indicates a balancing nature of them within the basin area. But the variation of mean and mean deviation of the relief classes between both sides of the RT signifies a dominant role of the RT to develop this Chal basin than the other thrust contacts of the area. The presence of a break in slope, the variation of lithology and relief between upper and middle fan area argues for the up thrusting of RT and formation of northward slanting Garubathan surface, which is not normal. Because the regional slope of the basin is southward. However, the headward erosion near MCT indicates its activeness, but the low intensity of the headward erosion to its western edge advocates for the higher effect of GTZ on relief than MCT in this part of the mountain area. This part of the mountain area is the footwall of GTZ, which decreases relief of the surface and resultant low intensity of headward erosion. The diagonal location of MFT with the southern margin of relief zone IV proves that the GTZ dominates over the MFT in the western margin of the lower basin area to control relief conditions. Like mountain area, this part of the study area is a footwall of the GTZ decrease surface height, which causes the extension of the relief zone IV through deposition and cross the MFT. Alternatively, the presence of headward erosion in the eastern side of the third relief zone advocates for tilting up (Fig: 4.b.c4) of the area due to the reactivation of MBT.

A great difference between _relative relief_ of the mountain surface from its southern alluvial plain refers to the high controlling nature of RT over relative relief. Presence of the highest relative relief zone near GTZ in the mountain area advocates for domination of GTZ over MCT. The distribution of _dissection index_ values implies that the RT sheet is erosive than the other part of the mountain area, which means that, presently this sheet supplies major sediments to the lower basin area. The presence of a patch of relative relief (20m-65m), slope (7°-17°), ruggedness index (0.7-0.9) and dissection index (0.10-0.26) zone near MBT refers to its reactivating nature.

Materials that are produced in headward erosion, are deposited in the distal lobe of the alluvial fan of the Chel basin. Thus, MBT plays a significant role in the alluvial fan expansion in the study area. The river terraces near MCT refer to its neotectonic activities. Thrustal up-warping of RT sheet (Fig: 3) near Grubathan market reduce slope (1°-7°) and resultant widening of Chal valley. The absence or negligible break in slope at MFT and MBT advocates less tectonic control of these thrusts than other thrust contacts (MCT, RT) of the study area.

5.2. Aspects of drainage basins

The heterogenic impact of tectonic movements segregates the basin surface into forty sub-basins. But, stretching of sub-basin 4, 24 and 26 across MCT, MFT, and MBT, respectively, direct the domination of geomorphic processes over tectonic control in those sub-basin areas. The development of a higher-order basin becomes possible in a relatively stable tectonic environment (Horton,1945). The maximum no of 3rd order sub-basin refers to a high degree of segregation of the Chel basin in a highly unstable tectonic environment (Horton, 1945). In the south of RT, a highly compressive nature of GTZ arrange the highly elongated 3rd and 4th order basin in both sides of the Chel river bank and its negligible effect causes the development of a vast and extensive 5th order sub-basin (No: 26) in the eastern part of the fan area. Alternatively, in the north of RT, the negligible effect of GTZ and MCT develops a relatively circular 5th order basin. But, between MCT and RT, the development of small sub-basins refers to RT neo-tectonics.

The distribution of the maximum values of *Ab, Pb, Lb, Wb, Lcm and Wcm* (Table: 3) also support the relatively higher neo-tectonic activeness of zone III than zone I (Table: 3). The circular basin shape is developed relatively in a stable tectonic condition than the elongated shape. Basin shape has a direct impact on the pic discharge of a stream. The highest pic discharge within a short period is greater in circular shape than the elongated shape (Morisawa, 1958; Wisler, C.O. and Brater, B.F. 1959; Gray, D. M. 1970; Bedient, P. B. et al. 1992). Thus, tectonics indirectly control basin processes like pic discharge, surface runoff, erosion, which controls the basin morphometry.

Distribution of *BSF, Eb* and *Rf* value refers to high tectonic pressure of GTZ that forms elongated sub-basins in zone IV and its relatively stable tectonic condition forms a circular sub-basin in the zone I. Distribution of K value refers to the tectonic stability of the Chel basin to its northern and southern margin. In an unstable tectonic environment, the steep slope and high relief tend the basin toward high *Re* value and vice-versa (Jaboyedoff, et al., 2011). In the study area presence of a circular sub-basin (*Re* is near to 1) in the mountain area and elongated basin (*Re* is <0.6) in the alluvial and flood plain area refers to the inactiveness of the MCT and active neo-tectonics of the GTZ. The same area may contain different lengths of perimeter due to the variation of geometric shape, which is the imprint of the neo-tectonics of that area. The values of *Rc* and *Kg* indicate that the highly elongated sub-basins of the region is experiencing high tectonic movement. The value of *Pr* and *Cc* announce that the tectonic pressure of this region gradually increases from north to south and decreases in the south of MFT.

5.3. Aspects of Stream Network

The development of a drainage network is the combined effect of climate, geology and neo-tectonics. The entire study area falls in the monsoon climate. Tectonic thrusts provide geological homogeneity to their north and south margins in the study area (Fig: 3). The variation of drainage networks in different parts of the same thrust zone advocates for higher domination of neotectonic than geology and climate over drainage. The tectonic controls the drainage morphometry directly by controlling basin morphometry and indirectly by controlling the distribution of geological formations, relief and slope. The highest order of stream implies tectonic stability for a long time and vice-versa (Horton,1945). So the development of 5th order circular sub-basin (1, 2 &10) refers to the tectonic stability of MCT. A low area of the highly elongated 3rd and 4th order sub-basins indicates the high compressive force of the GTZ. The distribution of 2nd order sub-basins refers to the RT neotectonics. Co-relations of the tectonic zone, *Nu, Lu* and *Lū* indicate the tectonic instability produced by GTZ. The distribution of *RLu, RLū, Rb, Rc* in the Chel basin is showing the tectonic instability between MCT and MBT. The concentration of the highest mean values of *Dt, Rt, If, Rw,* and *Rf* refers to the tectonic stability of the MCT, and the concentration of their minimum mean value in the RT-MBT tectonic zone refers to the presence of neo-tectonic activity in this area.

5.4. Chel river flow path

Frequent changes in the flow direction reveal the changing nature of the direction of neotectonic force neat the thrust contacts. A sedimentological study depicts that the change of flow direction from south-east to the south-west (Fig:14.b), from south-east to south (Fig:14.c) and from south-west to the south (Fig:14.d) are the neotectonic effect of RT, MBT and GTZ, respectively. The highest frequency of the river terraces near RT refers to its more neo-tectonic activeness than MCT. The lithological texture and internal organization of the upper terrace prove its development in the first phase in a neo-tectonic environment. The consequential development of river terraces is attributed to the series effect of tectonic movement in the study area. On the south of RT, the development of river terraces across MBT and MFT refers to the impact of GTZ from the western margin of the Chel basin. The sinuosity index of the Chel flow path indicates the negligible or absence of MFT neo-tectonics.

5.5. Lithology and Physical Properties of Sediment

The structurally uncommon thrusting of Garubathan formation over Darjeeling Gneiss (Fig:14.g) indicates the higher compressive nature of TR neo-tectonic than MCT. Near Garubathan market the highly scale-like foliated phyllaite of Garubathan formation reveals the gradual increasing pressure of neo-tectonics from north to south that advocates for the domination of RT neotectonics over MCT neo-tectonics. The rounded foothill boulders are either glacial or fluvial origin and the angular boulders are of tectonic origin (Basu, S.R., Sarkar, S., 1990). However, frequent effects of neo-tectonics cause the repetition of angular boulder layers in the south of RT. The high frequency of angular boulder facies near RT, reveals its activeness during the formation of the middle fan area. The angular boulder deposits with fine sediments in the floodplain area imply the tectonic instability of the catchment area that supplies the boulders, which are transported under high stream competency during the rainy season.

6. CONCLUSION

The overall observation depicts the tectonic variation in the Chel basin. Analysis shows that the RT and GTZ dominate over the MCT, MBT and MFT to attain this morphometry of this basin. The prominent break in slope, presence of highly foliated phyllaite and a great relief difference between upper and middle fan areas argued for active RT neo-tectonics. The highly elongated nature of the small sub-basin advocates for active neo-tectonic pressure of the GTZ from the western margin of the area. The presence of relatively large and higher-order circular sub-basins show the inactive nature of the MCT and MBT in the mountain and fan area, respectively. The sinuosity index indicates the inactive neo-tectonics of the MFT in the flood plain area. But, the presence of headword erosion sought for the reactivating nature of the MBT in the study area.

7. REFERENCES

1) Acharyya, S.K., (1971). Structure and stratigraphy of the Darjeeling Frontal zone, eastern Himalaya. In: Recent geological studies in the Himalaya, Geological Survey of India Miscellaneous Publication 24 (1), 71-90.

2) Acharyya, S.K., Ray, K.K., (1977). Geology of the Darjeeling–Sikkim Himalaya. Guide to Excursion No. 3, Fourth International Gondwana Symposium (Calcutta). Geological Survey of India, 1–25.

3) Basu, S.R., Sarkar, S., (1990). Development of alluvial fans in the foothills of the Darjeeling Himalayas and their geomorphological and pedological characteristics. In: Rachocki, A.H., Church, M. (Eds.), Alluvial Fans: A Field Approach. Wiley.

4) Beasom, S. L., E. P. Wiggers, and R. J. Giordono. (1983). A technique for assessing land surface ruggedness. Journal of Wildlife Management 47:1163–1166.

5) Bedient, P. B. and Huber, W. C. (1992). Hydrology and Floodplain Analysis (Second Edition). Addison – Wesley Publishing Company, New York.

6) Bhattacharya, S., (2004). Evolution and Characteristics of Alluvial Fans at the Foot Hills of the Darjeeling Himalayas, PhD Thesis, Department of Geography, University of Calcutta, Kolkata, 17-20, Accessed Library, Department of Geography, Vivekananda College for Women, Kolkata.

7) Bhattacharyya, K., and Mitra, G., (2009). A new kinematic evolutionary model for the growth of a duplex – an example from the Rangit duplex, Sikkim Himalaya, India. Gondwana Res., 16, 697–715. F: Earth Surf., 2011, 116, F03012; DOI: 10.1029/2010JF001841

8) Black, P. E. (1972). Hydrograph response to geometric model watershed characteristics and precipitation variables. Journal of Hydrology, 17, 309–329.

9) Burbank, D.W. and Anderson, R.S. (2001) Tectonic Geomorphology. Blackwell Scientific, Oxford, 274 p.

10) Chakraborty, Goswami C., Mukhopadhyay, D., Poddar, B.C., (2013). Geomorphology in relation to tectonics: a case study from the eastern Himalayan foothills of West Bengal. Quaternary International, 298, 80e92.

11) Chakraborty, S., Mukhopadhyay, S., (2014). A comparative study on the nature of channel confluence dynamics in the lower Jaldhaka River system, West Bengal, India. International Journal of Geology, Earth & Environmental Sciences, 4(2), 87e97.

12) Chakraborty, T., Ghosh, P., (2010). The geomorphology and sedimentology of the Tista megafan, Darjeeling Himalaya: implications for megafan building processes. Geomorphology, 115, 252e266.

13) Chandra, C.B. (2014): The Kaldiya River basin in Assam, Department of Geography, Gauhati

University; Access: Shodhganga: a reservoir of Indian theses @ INFLIBNET, http://hdl.handle.net/10603/73413

14) Chitra, C., Alaguraja, P., Ganeshkumari, K., Yuvaraj, D., Manivel, M. (2011). Watershed characteristics of Kundah sub-basin using remote sensing and GIS techniques. Int J Geomatics Geosci 2: 311–335.

15) Chorley, R. J., (1957). Illustrating the laws of morphometry, Geological Magazine, vol. 94, pp. 140-150.

16) Chow Ven T (1964). Handbook of applied hydrology. McGraw Hill Inc, New York.

17) Dasgupta, S., Pande, P., Ganguly, D., Iqbal, Z., Sanyal, K., Venkatraman, N.V., Dasgupta, S., Sural, B., Harendranath, L., Mazumdar, K., Sanyal, S., Roy, A., Das, L.K., Misra, P.S., Gupta, H., (2000). Sikkim Himalaya and Punea Basin, Plate SEISAT13. In: Nurula, P.L., Acharyya, S.K., Banerjee, J. (Eds.), Seismotectonic Atlas of India. Geological Survey of India, Kolkata.

18) De Smet (1951): Referred by Pal, S.S. (2091) in PhD thesis, Title: Landform and soil of a portion of Ajoy_Damodar interfluve West Bengal India, Chapter-VII; Department of Geography, The University of Burdwan, Access: Shodhganga: a reservoir of Indian theses @ INFLIBNET, http://hdl.handle.net/10603/68815

19) DeCelles, P. G., Gehrels, G. E., Quade, J. and Ojha, T. P., (1998). Eocene – early Miocene foreland basin development and the history of Himalayan thrusting, western and central Nepal. Tectonics, 17, 741–765

20) Dhalia, Md K., Ayazb, S., Sahanac, M., Guha, S., (2019); Response of sediment flux, bridge scouring on river bed morphology and geomorphic resilience in middle-lower part of river Chel, Eastern Himalayan foothills zone, India; Ecological Engineering, ELSEVIER B.V.; pp. 1-11

21) Dingman S. Lawrence, (2009) Fluvial Hydraulics, Oxford University Press, USA,

22) Doornkamp, J. C. and King, C. A. M., (1971). Numerical analysis in geomorphology- an introduction, Edward Arnold (Publishers) Ltd., GB. pp. 3-73

23) DovNir, (1957): The ratio of relative relief and absolute altitudes of Mt. Carmel: A Contribution to the problem of relief analysis and relief classification. Geog Rev. 47: 564 – 569

24) Elliot F.E. (1953): “A Technique of Presenting Slope and Relative Relief in One Map,” Surveying and Mapping, Vol. 13, Washington, pp. 473-478.

25) Faniran, A. (1968): The Index of Drainage Intensity - A Provisional New Drainage Factor. Australian Journal of Science. 31; 328-330.

26) Fergusson, J., (1863). Recent changes in the Delta of the Ganges. Journal of the Geological Society of London, 19, 321e354.

27) Gangopadhyay, P.K., Ray, S., (1980). Tectonic framework of the Rangit window around Namchi, South Sikkim. Himalayan Geology 10, 338-353.

28) Gansser, A., (1983). Geology of the Bhutan Himalaya, Birkhauser Verlag, Basel, p. 181.

29) Geddes, A., (1960). The alluvial morphology of the Indo-Gangetic plain: its mapping and geographical significance. Institute of British Geographers Transactions and Papers, 28, 253e276.

30) Ghosh, A.M.N., (1956). Recent advances in geology and structures of the Eastern Himalaya. Proceedings 43rd Indian Science Congress 2, 85-99.

31) Glock, W.S. (1932): “Available Relief as a Factor of Control in the Profile of a Landform”, Journal of Geography, Vol. 49, p. 74.

32) Gravelius, H., (1914): Grundrifi der gesamten Gewcisserkunde. B and I: Flufikunde (Compendium of Hydrology, Vol. I. Rivers, in German). Goschen, Berlin, Germany.

33) Gray, D. M. (1970). Handbook on the Principles of Hydrology. National Research Council of Canada.

34) Guha, D., Bardhan, S., Basir, S.R., De, A.K., Sarkar, A., (2007). Imprints of Himalayan thrust tectonics on the Quaternary piedmont sediments of the Neorae Jaldhaka Valley, DarjeelingeSikkim Sub-Himalayas, India. Journal of Asian Earth Sciences, 30, 464e473.

35) Hamdouni, R., Irigaray, C., Fernandez, T., Chacón, J. and Keller, E.A. (2007) Assessment of Relative Active Tectonics, Southwest Border of Sierra Nevada (Southern Spain). Geomorphology, 96, 150-173. http://dx.doi.org/10.1016/j.geomorph.2007.08.004

36) Heim, A. and Gansser, A., (1939) Central Himalayas, Geological observations of the Swiss Expedition of 1936, Memory of society Helveticae Science Nat 73, 1, 1-245

37) Horton, R. E. (1945). Erosional development of streams and their drainage basin: hydrological approach to quantitative morphology, Bulletin, Geological Society of America, vol. 56, pp. 275-370. http://dx.doi.org/10.1130/0016-7606(1945)56[275:EDOSAT]2.0.CO;2

38) Horton, R.E. (1932). Drainage Basin Characteristics. Transactions, American Geophysical Union, 13, 350-361. http://dx.doi.org/10.1029/TR013i001p00350

39) Jabbari, N., Servati, M.R. and Hosein Zadeh, M.M. (2012) The Study of Active Morphotectonic in Hesarak Basin (Northwest of Tehran) by Using Morphometric Indexes. Quantitative Geomorphological Researches, 2, 17-34.

40) Jaboyedoff, M., Giovanni B. Crosta & Stead, D. (2011): Slope Tectonics. Geological Society, London, Special Publications, 351, 1–10. DOI: 10.1144/SP351.1

41) Jagadeesh, J (1983): Landforms and settlements in Varada river basin, Department of Geography, Karnatak University; Access: Shodhganga: a reservoir of Indian theses @ INFLIBNET; http://hdl.handle.net/10603/108210

42) Kaberi, D. (2010): Terrain characteristics and their impact on land use of the Torsa-Raidak interfluve West Bengal, Department of Geography, University of Calcutta; Access: Shodhganga: a reservoir of Indian theses @ INFLIBNET; http://hdl.handle.net/10603/156040

43) Lama, S. and Maiti, R., (2019a): Morphometric Analysis of Chel River Basin, West Bengal, India, using Geographic Information System; Earth Science India; V. 12 (I), pp. 1-23.

44) Lama, S. and Maiti, R., (2019b): Morphometric Analysis of Chel River Basin, West Bengal, India, using Geographic Information System; Earth Science India; V. 12 (I), July 2019, pp. 1-23.

45) Lari, A. A.; Ansari, M. and Ansari, S. (2016). Analysis Neotectonic Activities in Khafr Basin, Journal of Geology, Scientific Research Publishing Inc. 6, 484-497. SciRes. http://www.scirp.org/journal/ojg http://dx.doi.org/10.4236/ojg.2016.66040

46) Lavé, J. and Avouac, J. P., (2001): Fluvial incision and tectonic uplift across the Hima layers of central Nepal. J. Geophys. Res. B: Solid Earth, 106(B11), 26561–26591.

47) Mandal, S., Sarkar, S. (2016). Overprint of neotectonism along the course of River Chel, North Bengal, India. Journal of Palaeogeography, 5(3), 221-240.

48) Mandi, S. and Soren, K., (2016) Morphotectonic Analysis of The Chel River Basin, Northern West Bengal, India; IOSR Journal of Humanities and Social Science (IOSR-JHSS) Volume 21, Issue 6, Ver. 7 PP 01-06

49) Matin, A., and Mukul, M., (2010): Phase of deformation from cross-cutting structural relationship in external thrust sheets: insight frontal small-scale structures in the Ramgarh thrust, Darjeeling Himalaya, Wes Bengal; Current Science, Vol.99, No.10

50) Mazumder, S. C. (1984): Geomorphology of Tripura, Department of Geography, North-Eastern Hill University; Access: Shodhganga: a reservoir of Indian theses @ INFLIBNET, http://hdl.handle.net/10603/61202

51) Melton, M.A., (1957): An Analysis of the Relations among the Elements of Climate, Surface Properties and Geomorphology. Technical Report 11, Department of Geology, Columbia University, New York.

52) Miller, V.C. (1953): A Quantitative Geomorphic Study of Drainage Basin Characteristics in the Clinch Mountain area, Virginia and Tennessee. Project NR 389-042, Technical Report: 3, Columbia University, Dept. of Geology, ONR, Geography Branch, New York.

53) Mitra, G., Bhattacharyya, K. and Mukul, M., (2010): The Lesser Himalayan Duplex in Sikkim: Implications for variations in Himalayan shortening. J. Geol. Soc. India, 75, 276–288.

54) Mohapatra, S.R.; Nayak, S.K.; Mohanty, A., Jana, P.; (2012): Geological section measurement study between Chel and Murti River, Jalpaiguri District, West Bengal.; GSI, Eartthquack Geology Division, Eastern region.; Report 2012

55) Molin P, Pazzaglia F J and Dramis F (2004) Geomorphic expression of active tectonics in a rapidly-deforming forearc, Sila Massif, Calabria, Southern Italy; Am. J. Sci. 304 559–589.

56) Morgan, J.P., McIntyre, W.G., (1959): Quaternary geology of the Bengal Basin, East Pakistan and India. Geological Society of America Bulletin, 70, 319e342.

57) Morisawa M E (1958): Measurement of drainage basin outline form, J. Geol, 66(5): 587–591.

58) Morisawa, M. I., (1962): Quantitative geomorphology of some watersheds in the Appalachian Plateau, Bulletin, Geological Society of America, vol. 73, pp. 1025-1046

59) Mukhopadhyay (1973,1977,1978a, 1978b and 1979c): Referred by Kaberi, D. (2010) in PhD thesis, Title: Terrain characteristics and their impact on land use of the Torsa-Raidak interfluve West Bengal, Chapter-VI; Department of Geography, University of Calcutta; Access: Shodhganga: a reservoir of Indian theses @ INFLIBNET; http://hdl.handle.net/10603/156040

60) Mukul, M. (2010): First-order kinematics of wedge-scale active Himalayan deformation: insights from Darjiling-Sikkim-Tibet (DaSiT) wedge. J. Asian Earth Sci. 39, 645-657. http://dx.doi.org/10.1016/j.jseaes.2010.04.029

61) Mukul, M., (2000): The geometry and kinematics of the Main Boundary Thrust and related neotectonics in the Darjiling Himalayan fold-and-thrust belt, West Bengal, India. Journal of Structural Geology 22(9), 1261-1283.

62) Mukul, M., Jade, S., Ansari, K. and Matim, A., (2014): Seismotectonic impact of strike-slip earthquakes in the Darjiling-Sikkim Himalaya, Current Science, Vol. 106, No. 2

63) Mukul, M., Jade, S., Matin, A., (2008): Active Deformation in the Darjiling-Sikkim Himalaya based on 2000-2004 Geodetic Global Positioning System Measurements. In Recent Advances in Earth Science: Indian Statistical Institute Platinum Jubilee Volumes, P.Ghosh & S. Bandyopadhyay (eds.), World Scientific Publisher, Singapore. 1-28.

64) Musy, A., (2001): Watershed Characteristic, In International Journal of Civil & Environmental Engineering IJCEE-IJENS Vol: 11 No: 06 http://citeseerx.ist.psu.edu/viewdoc/download?doi=10.1.1.661.9793&rep=rep1&type=pdf 19.102020 at 6.07 am and referred by Venkatesan, A. (2015) in PhD thesis, Title: Geoinformatics in fluvial geomorphological study of thoppaiyar sub-basin Tamil Nadu India, Chapter-VI; Department of Geography, Periyar University; Access: Shodhganga: a reservoir of Indian theses @ INFLIBNET; http://hdl.handle.net/10603/51184

65) Nakata, T., (1989): Active Faults of the Himalaya of India and Nepal. Geological Society of America, 232. Special Paper. 243-264.

66) Nir, D., (1957): "The Ratio of Relative Relief and Absolute Altitudes of Mt. Camel" Geographical Review. Vol. 47, p. 565.

67) Nir, D., (1957): Landform analysis of Mt. Kameral, Geographical Review, 47, pp.564.

68) Pandey, S. (1968): "Evolution of Hillslopes Around Jodhpur", National Geographical Journal of India, Vol. 14, Part-I, pp. 32-40.

69) Pareta, K. (2011). Geo-Environmental and Geo-Hydrological Study of Rajghat Dam, Sagar (Madhya Pradesh) using Remote Sensing Techniques, International Journal of Scientific & Engineering Research, 2(8) (ISSN 2229-5518), pp 1-8.

70) Partsch, J.S. (1911): Fine landeskunde fur das deiitche Volk Breslay. Map Faeing, 2: 568

71) Patel, P.P., (2012): Proceedings of State Level Seminar on Geographical Methods in the Appraisal of Landscape, held at Dept. of Geography, Dum Dum Motijheel Mahavidyalaya, Kolkata, on 20th March 2012, pp 1-14

72) Pearson, O. N. and DeCelles, P. G., (2005): Structural Geology and regional tectonic setting of the Ramgarh thrust, Himalayan fold-thrust belt of Nepal. Tectonics, 24. TC4008

73) Prasad, N., (1979) Hydrographic network and drainage basin analysis: a case study of the Barakar basin, Geographical Review of India, vol. 41 (4), pp. 297-303.

74) Rai, P. K., Chandel, R. C., Mishra, V. N. and Singh, P. (2018). Hydrological Inferences through Morphometric Analysis of Lower Kosi River Basin of India for Water Resource Management based on Remote Sensing Data, Applied Water Science (Springer), 8-15, pp. 1-16.DOI: https://doi.org/10.1007/s13201-018-0660-7.

75) Rai, P. K., Chandel, R. C., Mishra, V. N. and Singh, P. (2018). Hydrological Inferences through Morphometric Analysis of Lower Kosi River Basin of India for Water Resource Management based on Remote Sensing Data, Applied Water Science

(Springer), 8-15, pp. 1-16.DOI: https://doi.org/10.1007/s13201-018-0660-7.

76) Rai, P. K., Chaubey, P. K., Mohan, K. & Singh, P. (2017b). Geoinformatics for assessing the inferences of quantitative drainage morphometry of the Narmada Basin in India, Applied Geomatics (Springer), Vol. 9 (3), 1-23. DOI:10.1007/s12518-017-0191-1

77) Rai, P.K.*, Singh, P., Mishra, V. N., Singh, A., Sajan, B. and Shahi, A. P., (2019) Geospatial Approach For Quantitative Drainage Morphometric Analysis Of Varuna River Basin, India, Journal Of Landscape Ecology, Vol: 12 / No. 2, DOI: 10.2478/Jlecol-2019-0007

78) Rai, P.K., Mishra, V.N. & Mohan, K. (2017a). A Study of Morphometric Evaluation of the Son Basin, India Using Geospatial Approach, Remote Sensing Applications: Society and Environment, Vol. 7, 9-20. DOI: 10.1016/j.rsase.2017.05.001.

79) Raina, V.K., (1976): "The Rangit Tectonic Window"- stratigraphy, structure and tectonic interpretation and it's bearing on the regional stratigraphy. Proceedings of Himalayan Geology Seminar, New Delhi, 36-43.

80) Rais, S. & Javed, A. (2014). Drainage Characteristics of Manchi Basin, Karauli District, Eastern Rajasthan Using Remote Sensing and GIS Techniques. International Journal of Geomatics and Geoscience, Vol. 5 (1), pp. 285-299.

81) Raisz E. and Henry, J. (1937): An Average Slope Map of Southern New England, Geographical Review, Vol. 27, New York, pp. 467-472.

82) Ray, S., (1947) Zonal metamorphism in the eastern Himalayas and some aspects of local geology. Quarterly Journal of the Geological Mining and Metallurgical Society of India 19, 117–139.

83) Reitz, M. D., D. J. Jerolmack, and J. B. Swenson (2010), Flooding and flow path selection on alluvial fans and deltas, Geophys. Res. Lett., 37, L06401, doi:10.1029/2009GL041985.

84) Ritter, D.F., Kochel, R.C. and Miller, J.R. (1995) Process Geomorphology WBC/Mc Graw-Hill, Boston, 545 p.

85) Rosendahl, J., M. Vekic-slash, and J. Kelley (1993), Persistent selforganization of sandpiles, Phys. Rev. E, 47(2), 1401–1404, doi:10.1103/ PhysRevE.47.1401.

86) Sambrook Smith, G., and R. Ferguson (1995), The gravel-sand transition along river channels, J. Sediment. Res., 65(2), 423–430.

87) Savenije, H. (2003), The width of a bankful channel; Lacey's formula explained, J. Hydrol., 276, 176–183, doi:10.1016/S0022-1694(03)00069-6.

88) Schideggar. A.E., (1970): Theoretical Geomorphology. 2nd edn. Berlin-Heidelberg New York: Springer.

89) Schumm, S., M. P. Mosley, and W. E. Weaver (1987), Experimental Fluvial Geomorphology, John Wiley, New York.

90) Schumm, S.A. (1956) Evolution of Drainage Systems and Slopes in Badlands at Perth Amboy, New Jersey. Geological Society of America Bulletin, 67, 597-646. http://dx.doi.org/10.1130/0016-7606(1956)67[597:EODSAS]2.0.CO;2

91) Sharma, H.S. (1981): Perspective in Geomorphology, Concept Publishing Company, Vol. IV, New Delhi, p-81.

92) Sheets, B., T. Hickson, and C. Paola (2002), Assembling the stratigraphic record: Depositional patterns and time-scales in an experimental alluvial basin, Basin Res., 14, 287–301, doi:10.1046/j.1365-2117.2002.00185. x.

93) Singh and Singh, (1997) in Kuldeep Pareta1, Upasana Pareta2 (2011): Quantitative Morphometric Analysis of a Watershed of Yamuna Basin, India using ASTER (DEM) Data and GIS, International Journal Of Geomatics And Geosciences, Volume 2, No 1, 248-269

94) Singh, K. N. (1980). Quantitative analysis of landforms and settlement distribution in southern uplands of eastern Uttar Pradesh (India).

95) Singh, P., Thakur, J. & Singh U. C. (2013). Morphometric analysis of Morar River Basin, Madhya Pradesh, India, using remote sensing and GIS techniques. Environ Earth Sci 68:1967–1977

96) Singh, S., & Dubey, A. (1994). Geo-environmental planning of watersheds in India. Allahabad: Chugh Publications.

97) Slingerland, R., and N. Smith (2004), River avulsions and their deposits, Annu. Rev. Earth Planet. Sci., 32, 257–285, DOI: 10.1146/annurev. earth.32.101802.120201.

98) Slmith, G.H. (1935): The relative relief of Ohio. Geographical Review, 25: 272 – 84

99) Smith, G. H. (1935): The relative relief of Ohio, Geographical Review, Vol.25, pp.272-84

100) Smith, K.G. (1950) Standards for Grading Textures of Erosional Topography. American Journal of Science, 248, 655-668. http://dx.doi.org/10.2475/ajs.248.9.655

101) Smith, N. D., T. A. Cross, J. P. Dufficy, and S. R. Clough (1989), Anatomy of an avulsion, Sedimentology, 36, 1–23, doi:10.1111/j.1365-3091.1989.tb00817.x.

102) Srivastava, P. and Mitra, G., (1994): Thrust geometries and deep structure of the outer and lesser Himalaya, Kumaon and Garhwal (India): implications for evolution of the Himalayan fold-and-thrust belt. Tectonics, 13, 89–109.

103) Srivastava, V., Manas Mukul, M., Mukul, M.*, (2017) Quaternary deformation in the Garubathan recess: Insights on the structural and landscape evolution in the frontal Darjiling Himalaya. Elsevier Ltd and Quaternary International No.462; pp.138-161.

104) Starkel, L., Sarkar, S., Soja, R. and Prokop, P., (2008): Present-Day Evolution of the Sikkimese-Bhutanese Himalayan Piedmont, Geographical Studies: No. 219; Instytut Geografii i Przestrzennego Zagospodarowania PAN im. Stanisława Leszczyckiego, Warszawa; PL ISSN 0373-6547; ISBN 978-83-61590-09-5 https://www.researchgate.net/publication/261196285_Present-day_evolution_of_the_Sikkimese-Bhutanese_Himalayan_Piedmont/link/0c96053393bc36e14c000000/download ; Access on 19.10.2020 at 3.15a.m

105) Strahler, A.H., (1964): Quantitative Geomorphology of Drainage Basins and Channel Networks in Handbook of Applied Hydrology, McGraw Hill Book Company, Newyork, Section 4, pp 39-76.

106) Strahler, A.N. (1952a) Dynamic Basis of Geomorphology. Geological Society of America Bulletin, 63, 923-938. http://dx.doi.org/10.1130/0016-7606(1952)63[923:DBOG]2.0.CO;2

107) Strahler, A.N. (1952b) Hypsometric (Area-Altitude) Analysis of Erosional Topography. Geological Society of America Bulletin, 63, 1117-1142. http://dx.doi.org/10.1130/0016-7606(1952)63[1117:HAAOET]2.0.CO;2

108) Strahler, A.N. (1956) "Quantitative Slope Analysis". Bulletin of the Geological Society of America, Vol. 67, New York, pp. 571-596.

109) Strahler, A.N., (1958) Dimensional analysis applied to fluvially eroded landforms: Geol. Soc. Am. Bull., v. 69, p. 279-300.

110) Surkan, (1967): referred by Yadav, B. (2019) in PhD thesis, Title: Fluvial Geomorphology of Basna Drain and Mansaita River with Special Reference to Settlement and Agriculture A Case Study of Phaphamau Environs, Chapter-III; Department of Geography, University of Allahabad; Access: Shodhganga: a reservoir of Indian theses @ INFLIBNET; http://hdl.handle.net/10603/270181

111) Trewartha, G.T. (1957): New Population Maps of Uganda, Kenya, Nyasaland, And Gold Coast; Annals of the Association of American Geographers; Volume47, Issue1, Pages 42-58. https://doi.org/10.1111/j.1467-8306.1957.tb01522.x

112) Valdiya, K. S., (2002): Emergence and evolution of Himalaya: reconstructing history in the light of recent studies, Progress in Physical Geography 26,3 pp. 360–399

113) Verstappen, H. (1983). The Applied Geomorphology. International Institute for Aerial Survey and Earth Science (I.T.C), Enschede, The Netherlands. Amsterdam, Oxford, New York.

114) Wentworth, C.K. (1930): "A Simplified Method of Determining the Average Slope of Land Surfaces", American Journal of Science, Series 5, Vol. 20, New Haven, Conn.

115) Wisler, C.O. and Brater, B.F. (1959): Hydrology; John Wiley & Sons Inc, Ed:1st; New York; ISBN-13: 978-0471956341

116) Yin, A., (2006): Cenozoic tectonic evolution of the Himalayan orogen as constrained by along-strike variation of structural geometry, exhumation history, and foreland sedimentation. Earth-Sci. Rev., 76, 1–131.